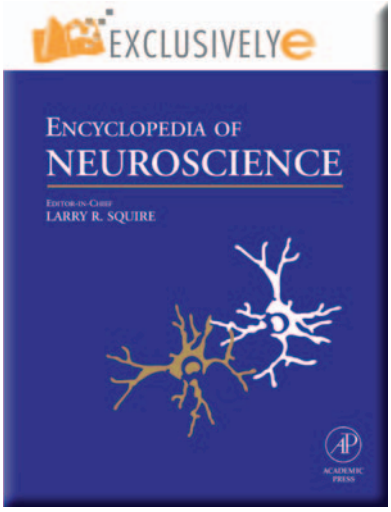

Kawato M (2009) Cerebellum: Models. In: Squire LR (ed.) Encyclopedia of Neuroscience, volume 2, pp. 757-767. Oxford: Academic Press.

Cerebellum: Models

M Kawato, ATR Computational Neuroscience Laboratories, Kyoto, Japan

Cerebellar Learning Models

The cerebellum is one of the best- and earliest-studied parts of the brain. In the past 50 years, a number of conceptual models have proposed various functions, such as error correction, coordination, timing processing, and rhythm. Among these, cerebellar learning models have always been the most attractive, versatile, and influential. They are also the most explicit class of theory from the computational viewpoint. A large number of experiments and theoretical studies have been conducted to resolve the controversies and disputes surrounding them. The learning models are based on unique structures of the cerebellar cortex. The Purkinje cell, the only output neuron in the cerebellar cortex, receives two major excitatory inputs from climbing fibers and parallel fibers. A single climbing fiber axon makes multiple synapses on a single Purkinje cell and induces very strong excitatory postsynaptic potentials, which lead to complex spikes that consist of a few Ca^{2+} spikes. By contrast, 200 000 synapses from parallel fibers, which are the axons of 10^{10-11} granule cells, generate simple spikes, each of which is a single Na^{+} spike.

Brindley first proposed that parallel fiber–Purkinje cell synapses undergo plastic changes if the climbing fiber input is concomitantly activated. Around 1970, Marr, Albus, and Ito postulated the first learning theory of the cerebellar neural circuits. Albus correctly predicted that synaptic efficacy decreases if the parallel and climbing fibers are simultaneously activated, which was later physiologically demonstrated as long-term depression (LTD) by Ito and colleagues. Ito proposed that the climbing fiber input carries an error signal rather than a teacher (desired output) signal and explained adaptation of the vestibulo-ocular reflex by an LTD-based learning model.

A general model of cerebellar learning, which is an extension of the model proposed by Ito to explain general movements with many degrees of freedom and a simplification of the model proposed later by Kawato, is shown in Figure 1. Mossy fiber inputs carry information on the goal of a movement, sensory feedback about the current state of the body and the external world, and the efference copy of motor commands to granule cells. Purkinje cells, mainly activated by parallel fiber inputs from granule cells, project to cerebellar nuclei, which further transmit information to downstream motor systems such as the oculomotor system, spinal cord, red nucleus, and cerebral cortex via the thalamus (depicted together as the postcerebellar network in Figure 1). Motor commands generated by this network induce movements, which are measured by sensory organs. Subtracting this measured state feedback to the brain from the desired state gives the sensory error, which is further transformed into the appropriate coordinates for Purkinje cell outputs. The inferior olive neurons send this transformed error back to Purkinje cells via the climbing fibers.

Cerebellar Purkinje cell learning can be modeled by the following simple supervised learning based on the known synaptic plasticity of parallel fiber–Purkinje cell synapses, including LTD and long-term potentiation (LTP), and the rebound potentiation of inhibitory synapses on Purkinje cells, as well as LTP between parallel fibers and inhibitory interneurons. For simplicity, the firing rate $-y$ of a Purkinje cell is assumed to be the weighted summation of 200 000 parallel fiber inputs x_i:

$$-y = \sum_{i=1}^{200\,000} w_i x_i$$

Then, the inhibitory action on deep cerebellar nuclei is negative of the Purkinje output, y. If the desired output for the sign-inverted Purkinje cell's simple spike is denoted as y_d, then the objective function to be minimized for the supervised learning, in which the synaptic weight w_i is learned so that the actual output y best approximates the desired output y_d, is given as

$$E = 1/2(y_d - y)^2$$

The steepest descent direction of this error function can be obtained by the following partial derivative (called the Widrow–Hoff rule):

$$\Delta w_i, \propto -\frac{\partial E}{\partial w_i} = -\left(-\frac{\partial y}{\partial w_i}\right)(y_d - y) = -x_i(y_d - y)$$
$$= -x_i(C - \bar{C})$$

Here, $(C - \bar{C})$ is the difference between the climbing fiber firing rate and its temporal average (background firing activity), and it is assumed to encode the error signal in the last equation.

When both parallel and climbing fibers are activated, x_i and $(C - \bar{C})$ are positive, and thus Δw_i is negative (LTD). In contrast, when the parallel fiber is activated and the climbing fiber is not, then

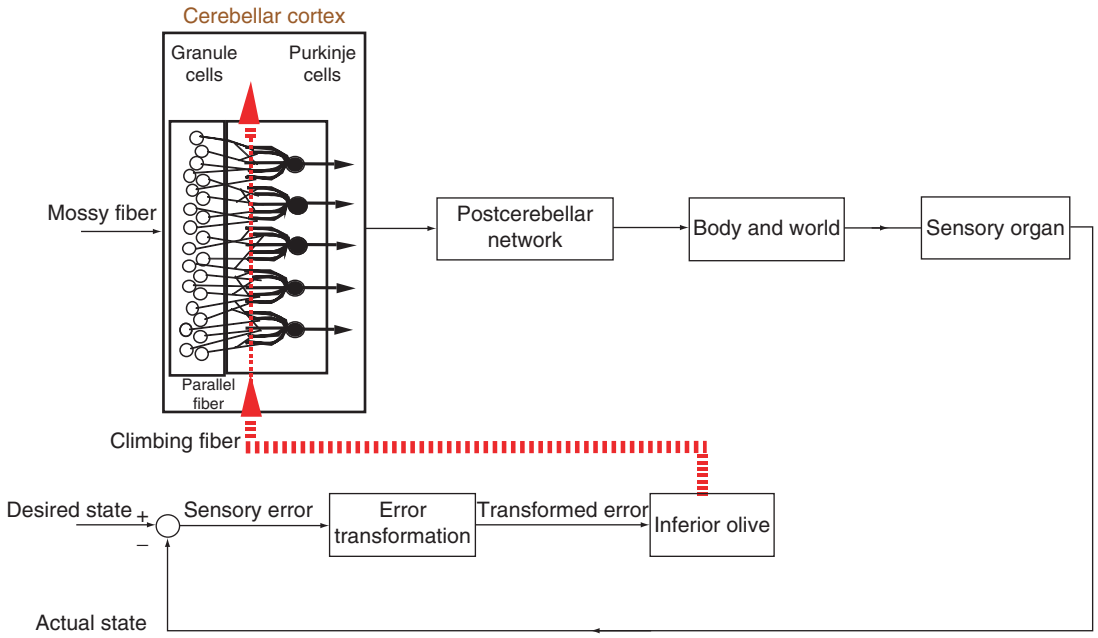

Figure 1 A cerebellar learning model.

x_i is positive but $(C-\bar{C})$ is negative, and thus Δw_i is positive (LTP). When both the climbing fiber and the inhibitory interneuron synapse on a Purkinje cell are activated, x_i and $(C-\bar{C})$ are positive, and thus Δw_i is negative, leading to an increase in the amplitude of w_i, which is negative (LTP of inhibitory pathway).

Cerebellar learning theory predicts that a memory of learning is stored at parallel fiber–Purkinje cell synapses; that LTD is an elementary cellular process of cerebellar learning; and that climbing fibers carry an error signal with some precision in the output coordinates of Purkinje cells. These predictions have all stimulated a vast amount of experimental examination and controversy, but they have been quite well supported by recent data and modeling four decades after they were first proposed. These controversial issues are discussed below.

It is well established that when the cerebellum as a whole is lesioned, for some movements, learning capability is lost, stored memory of learning is destroyed, and movements are not well corrected or coordinated. Controversies have centered mainly on the question of whether the cerebellar cortex (Purkinje cell synapses) or the cerebellar nucleus is the major site of memory. Recent systematic lesion studies have shown that the cerebellar cortex is a memory site for several days at least and that the cerebellar nuclei can contain even longer memory. Interfering with LTD pharmacologically (e.g., by administration of hemoglobin, which is a scavenger of NO, essential for LTD) or by genetic manipulation (knockout mice and their pharmacological rescue) are more recent and sophisticated ways of resolving this controversy. Abolishment of LTD was shown to destroy various motor learning capabilities, such as adaptation of walking, vestibulo-ocular reflex, optokinetic eye movements, and precise timing in eyeblink conditioning.

Computational Models of Cerebellar LTD

If LTD of parallel fiber–Purkinje cell synapses is the elementary cellular process of supervised learning, as postulated in the cerebellar learning theory, it must satisfy the following three requirements. First, LTD should be associative. That is, LTD should be induced only when both parallel fiber inputs and climbing fiber inputs are conjunctively activated. Second, LTD should be maximally induced when climbing fiber activation is delayed 50–200 ms with respect to parallel fiber activation. This is because the time window of LTD should compensate for the delay of the reafferent climbing fiber inputs to feedback the consequences of the parallel fiber–simple spike-induced movements. Third, LTD should be synapse specific; only a parallel fiber synapse that is conjointly activated with a climbing fiber input should be depressed, but not other synapses. However, a considerable number of studies have reported violations of these three requirements under some experimental conditions; consequently, LTD has been questioned several times as the elementary process of cerebellar supervised learning and has been postulated for other functions, such as the

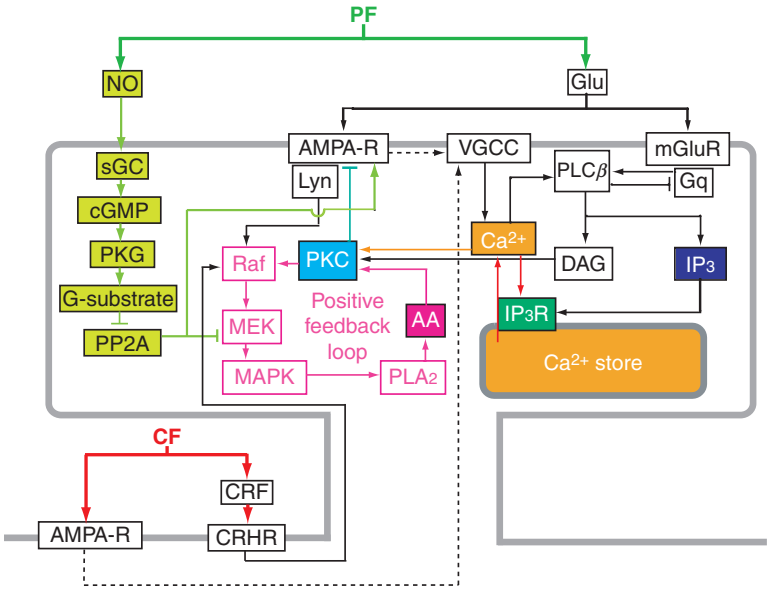

Figure 2 Signal transduction model of cerebellar long-term depression. AA, arachidonic acid; AMPA-R, α-amino-3-hydroxy-5-methyl-4-isoxazole propionic acid receptor; CF, climbing fibers; cGMP, cyclic guanosine monophosphate; CRF, corticotropin releasing factor; CRHR, the human corticotropin releasing factor; DAG, diacylglycerol; Glu, glutamate; Gq, G-proteins; IP_3, inositol 1,4,5-triphosphate; IP_3Rs, IP_3 receptors; MAPK, mitogen-activated protein kinase; MEK, MAP/extracellular signal-regulated kinase; mGluR, metabotropic glutamate receptor; NO, nitric oxide; PF, parallel fibers; PKC, protein kinase C; PKG, cGMP-dependent protein kinase; PP2A, protein phosphatase 2A; PLA_2, cytosolic phospholipase A_2; PLCβ, phospholipase Cβ; sGC, soluble guanylyl cyclase; VGCC, voltage-gated calcium channel.

normalization of total synaptic efficacies on a single Purkinje cell. The kinetic simulation model of LTD signal transduction pathways in a Purkinje cell dendritic spine (Figure 2) provides a coherent perspective on these confusing experimental data and competing theoretical hypotheses, and it is described below.

Climbing fiber inputs activate α-amino-3-hydroxy-5-methyl-4-isoxazole propionic acid (AMPA) receptors (AMPA-Rs) on dendritic shafts and induce depolarization, which opens the voltage-gated calcium channels (VGCCs), as indicated by the broken line in Figure 2, leading to Ca^{2+} influx from the extracellular space into the spine head, reaching a concentration of about $1\,\mu mol\,l^{-1}$. Parallel fiber inputs also induce AMPA-R activation on dendritic spines, just as a climbing fiber input does, but parallel fiber inputs produce smaller depolarization and Ca^{2+} influx. In addition, they simultaneously activate metabotropic glutamate receptors (mGluRs). Furthermore, they presynaptically synthesize nitric oxide (NO), which diffuses into the spine. In the metabotropic pathway, activated mGluRs induce production of inositol 1,4,5-trisphosphate (IP_3) and diacylglycerol via G-proteins and phospholipase Cβ at the postsynaptic density. IP_3 then diffuses into the cytosol and binds to IP_3 receptors (IP_3Rs), which are IP_3-gated Ca^{2+} channels on the intracellular Ca^{2+} stores, such as endoplasmic reticulum (ER). Cytosolic Ca^{2+} above some threshold triggers a regenerative cycle of IP_3-dependent Ca^{2+}-induced Ca^{2+} release (depicted as a positive feedback loop between Ca^{2+} and IP_3Rs in Figure 2) from the ER via IP_3Rs opened by binding of both IP_3 and Ca^{2+}. This means that the open probability of IP_3Rs increases with Ca^{2+} concentration, and the Ca^{2+} threshold of this regenerative cycle decreases with IP_3 concentration. An increase in cytosolic IP_3 concentration was simulated to be maximal at $3\,\mu mol\,l^{-1}$ about 100 ms after the parallel fiber input. This slow rate of increase in IP_3 concentration is due to the slow dynamics of the metabotropic pathway. Because Ca^{2+} influx via VGCCs due to climbing fiber activation is an immediate event, when the climbing fiber input is delayed about 100 ms with respect to the parallel fiber input, Ca^{2+} increase coincides with IP_3 increase, and they together trigger the Ca^{2+}-induced Ca^{2+} release of $10\,\mu mol\,l^{-1}$. If either climbing fiber input or parallel fiber input alone is activated, this large Ca^{2+} release does not occur because either IP_3 or Ca^{2+}, respectively, does not reach the threshold for the regenerative cycle. Consequently, the Ca^{2+} nonlinear excitable dynamics model by Doi (right third of Figure 2) reproduced the associative nature and the spike timing-dependent plasticity (STDP) of LTD.

In the model proposed by Kuroda, the large Ca^{2+} increase, which is caused by the conjunctive parallel fiber input and the delayed climbing fiber input, induces

the activation of linear cascades of phosphorylation of protein kinase C (PKC), followed by phosphorylation and then internalization of AMPA-R, which explains the early phase of LTD up to about 10 min. On the other hand, the intermediate phase of LTD, up to several times longer, is mediated by a mitogen-activated protein (MAP) kinase-dependent positive feedback loop, which consists of PKC, Raf, MAP/extracellular signal-regulated kinase (MEK), MAP kinase, cytosolic phospholipase A_2, arachidonic acid, and back to PKC (Figure 2). This positive feedback loop has two stable equilibrium points separated by a saddle point that determines the threshold of LTD. At the low equilibrium point, the MAP kinase positive feedback loop is not activated, but if strong and long Ca^{2+} elevation occurs, the state jumps to the higher equilibrium over the saddle point, and AMPA-Rs continue to be phosphorylated and internalized during this prolonged activation of the positive feedback loop. Consequently, this MAP kinase positive feedback model (middle third of Figure 2) explains the long-term nature of LTD and is supported by George Augustine, Keiko Tanaka, and collaborators.

In the Kuroda model (left third of Figure 2), NO activates soluble guanylyl cyclase (sGC), and the activated sGC catalyzes the conversion of guanosine triphosphate into cyclic guanosine monophosphate (cGMP), which activates cGMP-dependent protein kinase (PKG). PKG phosphorylates its substrate, G-substrate, and phosphorylated G-substrate preferentially inhibits protein phosphatase 2A (PP2A). Activated PP2A dephosphorylates MEK and AMPA-R. Inhibition of the dephosphorylation of MEK was required for the activation of the MAP kinase positive feedback loop. Therefore, by ultimately inhibiting PP2A and activating the positive feedback loop, NO plays a permissive role in the induction of LTD.

The Ca^{2+} dynamics model coherently reproduces both the associative and the nonassociative natures of LTD and the spike timing dependency of associative LTD as follows. Within the physiological ranges of input strength, the conjunctive stimulation of the parallel fiber input and the delayed climbing fiber input is essential to induce a large, regenerative Ca^{2+} increase, which is necessary for crossing the threshold of the MAP kinase positive feedback loop and inducing LTD. However, if stimulation of parallel fiber bundles is strong enough, or if uncaged Ca^{2+} or IP_3 is abundant enough, these stimuli alone can increase the Ca^{2+} concentration so that it crosses the Ca^{2+} dynamics threshold, resulting in a large enough Ca^{2+}-induced Ca^{2+} release from the ER to reproduce nonassociative LTD. In the hippocampal and cerebral pyramidal neurons, backpropagation of somatic action potentials releases the magnesium block on *N*-methyl-D-aspartate (NMDA) receptors and is the essential mechanism for millisecond-order STDP there. Backpropagation of somatic action potentials requires activity of postsynaptic cells, which is the essential condition of Hebbian learning. Neither backpropagation nor the NMDA receptors exist in Purkinje cells, suggesting cellular mechanisms for the clear distinction of Purkinje cell-supervised learning, with 100-ms STDP, from cerebral Hebbian learning, with STDP of tens of milliseconds.

The excitable dynamics of the Ca^{2+} model and bistable dynamics of the MAP kinase positive feedback loop model may provide a possible molecular mechanism to resolve the 'plasticity–stability' dilemma of memory stability with environmental sensitivity. Each spine is equipped with a surprisingly small number of molecules (e.g., only tens of AMPA-Rs). With a cascade of excitable and bistable dynamics starting from Ca^{2+} dynamics, followed by the MAP kinase positive feedback loop, internalization of AMPA receptors, a possible change in cytoskeleton and membrane proteins, and finally a morphological change in the spine, LTD can be induced by very delicate and low-energy inputs but acquired memory can be maintained over a prolonged period of days, even under stochasticity due to the small numbers of molecules.

The synapse specificity of LTD is also well explained by the NO model combined with an electrical cable model of Purkinje cell dendrite and spines, the Ca^{2+} dynamics model, and the MAP kinase positive feedback loop model. When no nearby parallel fiber is activated and NO is low, even a conjunction of the parallel fiber and climbing fiber inputs cannot induce LTD. If too many surrounding parallel fibers are stimulated and NO is very high, even the synapse, which is not stimulated, exhibits LTD only by climbing fiber stimulation. In this case, a spread of LTD occurs, and the synapse specificity of LTD is lost. Only when a modest number of parallel fibers are activated and NO is within an intermediate range can synapse-specific LTD occur; the contextual information for storing different motor skills might be conveyed by this gating mechanism. This strongly predicts the sparseness of parallel fiber coding *in vivo*, which has recently gained much experimental support.

Altogether, the LTD kinetic simulation models provide a comprehensive account of several seemingly diverse, conflicting, and unrelated experimental data within the framework of complicated nonlinear dynamics regulated by Ca^{2+}, IP_3, and NO concentrations. We must note that because of the nonlinear summation effects of these signaling molecules, nonphysiological stimuli *in vitro*, such as parallel fiber bundle stimulation, uncaging of Ca^{2+}, and IP_3, might induce characteristics qualitatively different

from those induced *in vivo* LTD in terms of its associative nature, spike timing dependency, and synapse specificity.

Rhythmic versus Chaotic Firing of Inferior Olive Neurons

The most influential model of the cerebellum other than the learning theory is probably the timing, rhythm, and synchronization hypothesis. The inferior olive nucleus, which sends out climbing fibers to Purkinje cells, possesses the highest density of gap junctions in the mammalian brain. Inferior olive neurons have several unique ion channels distributed on the somatic and dendritic membrane, as shown in Figure 3(a), and these exhibit rhythmic activities in slice preparation under some conditions, especially with harmaline. However, in awake monkeys at rest, no rhythmicity has been found for complex spikes. When the effective electrical conductance of gap junctions is increased by picrotoxin application to the inferior olive, which blocks inhibitory synapses on glomeruli of inferior olive neurons from cerebellar nuclei, the inferior olive neurons tend to be spatially synchronized in their firing.

None of these unique and well-studied anatomical and physiological characteristics of inferior olive

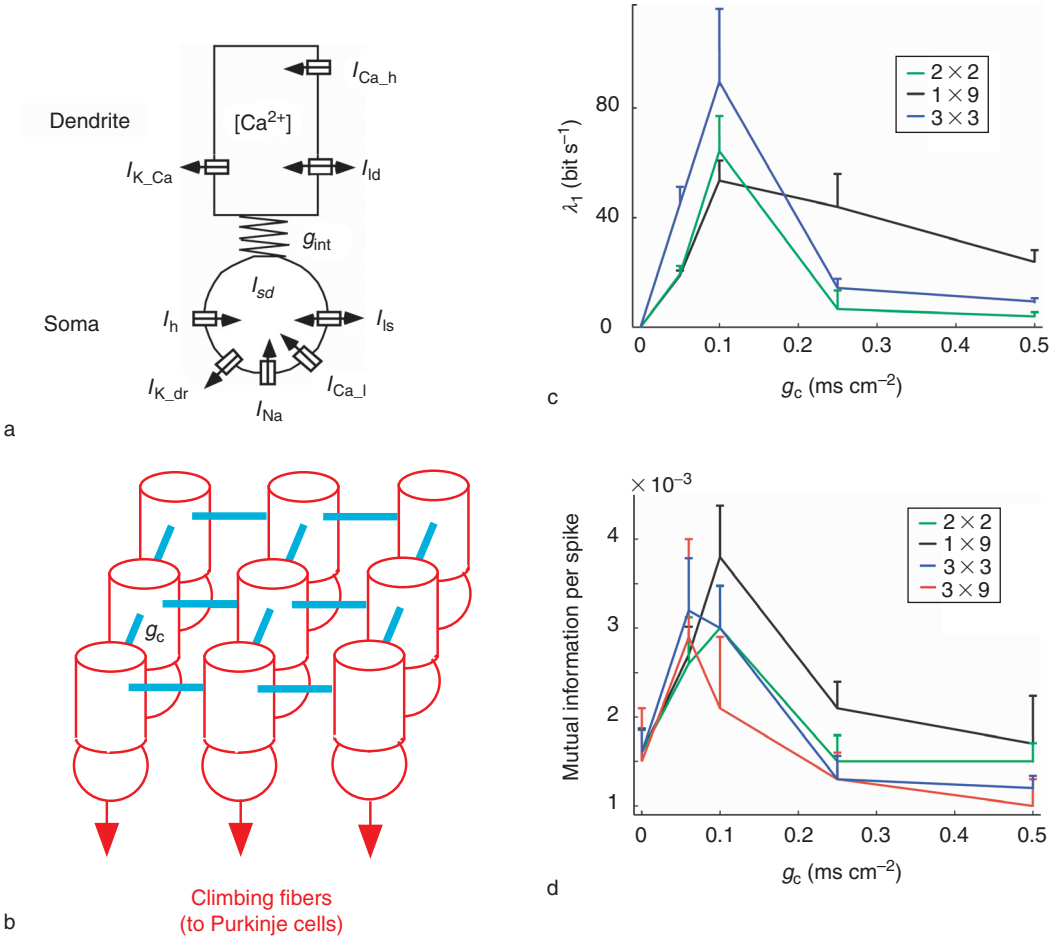

Figure 3 A network model of inferior olive (IO) neurons electrically connected by gap junctions. (a) Two-compartment biophysical model of an IO cell. The somatic ionic currents include a low-threshold calcium inward current (I_{Ca_l}), an anomalous inward rectifier current (I_h), the Hodgkin–Huxley type inward sodium (I_{Na}) and outward delayed rectifier potassium (I_{K_dr}) currents, and a leakage current (I_{ls}). The dendritic currents include a high-threshold inward calcium current (I_{Ca_h}), an outward calcium-dependent potassium current (I_{K_Ca}), and a leakage current (I_{ld}). As the dendritic potassium current I_{K_Ca} is calcium dependent, Ca^{2+} concentration dynamics is included in the model. g_{int} is the coupling conductance between the two compartments and I_{sd} is the current flowing through this conductance. The electronic coupling between this cell and multiple other cells is not shown. (b) Between 4 and 27 IO cells are connected on a lattice by electrical conductance via gap junctions; g_c, coupling strength. (c) Largest Lyapunov exponent as a function of g_c for different networks of nonidentical cells. Error bars are standard deviations obtained from 10 different simulations. When the largest exponent was large, the network exhibited marked chaotic behavior. When the largest exponent was close to zero, firing was almost rhythmic. (d) Network mutual information per spike as a function of g_c for different networks of nonidentical cells. Adapted from Schweighofer N, Doya K, Fukai H, Chiron JV, Furukawa T, and Kawato M (2004) Chaos may enhance information transmission in the inferior olive. *Proceedings of the National Academy of Sciences of the United States of America* 101: 4655–4660, with permission from National Academy of Sciences, USA.

neurons has been incorporated into or explained by the learning theory until recently. Schweighofer and colleagues developed a two-compartment model of an inferior olive neuron, as shown in Figure 3(a), with known spatial distribution of ion channels. These neurons are connected by gap junctions within a planar sheet, as shown in Figure 3(b), and the firing characteristics, as well as the input and output information transfer characteristics, have been examined. The network model reproduced rhythmic firing, as well as synchronized oscillation, when the coupling conductance was high. Figure 3(c) plots the largest Lyapunov exponent of the network dynamics as a function of the coupling conductance. The small Lyapunov exponent at large conductance indicates that the firing is synchronized and rhythmic when electrical coupling is strong, corresponding to picrotoxin application. With small conductance, each neuron periodically fires at its own frequency without much interaction; thus, the Lyapunov exponent is again close to zero, indicating an almost periodic solution. However, with medium conductance, the Lyapunov exponent is much higher than zero, indicating that neurons fire asynchronously and aperiodically. This is actually chaotic and desynchronized firing, and for this range of dynamics, input and output information transmission becomes the largest, as shown in Figure 3(d). These theoretical predictions were recently supported experimentally. Consequently, climbing fiber inputs can convey error signals most efficiently, even with their low firing frequency (typically 1 spike s^{-1}), when the conductance is medium and chaos is induced. Low-frequency firing usually implies poor representation of the error signal. Chaotic and desynchronized firing of inferior olive neurons might be a basic neural mechanism for insuring high-fidelity error-signal transmission even with a low firing rate.

The feedback error learning theory of the cerebellum explained in the next section theoretically requires low firing rates of climbing fiber inputs. This is because climbing fiber inputs convey time-delayed feedback motor commands, and if they were to be strongly manifested in Purkinje cell output, smooth and sophisticated feed-forward motor control would be ruined. Hirano and his colleagues provided experimental support for this prediction in AMPA-R delta 2 knockout mouse. Climbing fiber inputs occupy a much larger proportion of Purkinje cell output in this knockout mouse compared with a normal mouse, and optokinetic eye movements are much more delayed than is control performance.

Feedback Error Learning Model

Although early learning models proposed that the cerebellum conducts pattern recognition, probably influenced by a 'perceptron,' they are not consistent with physiological data showing that simple spike firing rates of Purkinje cells temporally change and encode dynamic and kinematic features of movements. Recent studies suggest that the human cerebellum is important for sensory and cognitive functions as well as for motor control. What general computation might be realized by the cerebellar cortex that would cover the sensory, cognitive, and motor domains; would be compatible with existing hypotheses, such as timing, coordination, and error correction; and could be learned by supervised learning such as that shown in Figure 1? Internal models seem to provide the most versatile and compatible computational entity satisfying all these requirements. Internal models are neural networks inside the brain ('internal') that can mimic ('model') the input–output characteristics of some dynamic process outside the brain. In a motor control context, a forward model of a body can predict sensory consequences of movement from the efference copy of a motor command. This is because the controlled objects in movements generate a trajectory from motor commands. By contrast, the inverse model of a body and the external world can compute the necessary motor commands from a desired movement pattern. Internal models are useful for predictive computations in sensory, cognitive, and motor functions. If an inverse dynamics model for a controlled object possessing dynamics and kinematics with multiple degrees of freedom is destroyed, the movement becomes clumsy, slow, and not well corrected, because neither feed-forward nor feedback control (both of which are dependent on the inverse model) is available. Thus, control must rely on poor and crude feedback control alone. Internal models can be learned based on supervised learning.

Around 1990, Kawato proposed that different parts of the cerebellum contain either forward or inverse models. He also proposed a computational scheme called feedback error learning to acquire an inverse model in the supervised learning scheme, as shown in Figure 4(a). If supervised learning takes place in the brain for motor control, the following difficult computational problem called 'distal teacher,' formulated by Jordan, should be resolved. As shown in Figure 1, the error between desired and actual movement patterns can be measured by sensory organs, but these movement errors could be very different in spatial coordinates as well as in temporal dynamics from the necessary error signal for the motor command. Furthermore, it should be emphasized that there exists no teaching signal for motor commands in supervised motor learning, because if it were to exist, it would be directly utilized for motor control, and there would be no need for learning. The distal teacher problem is

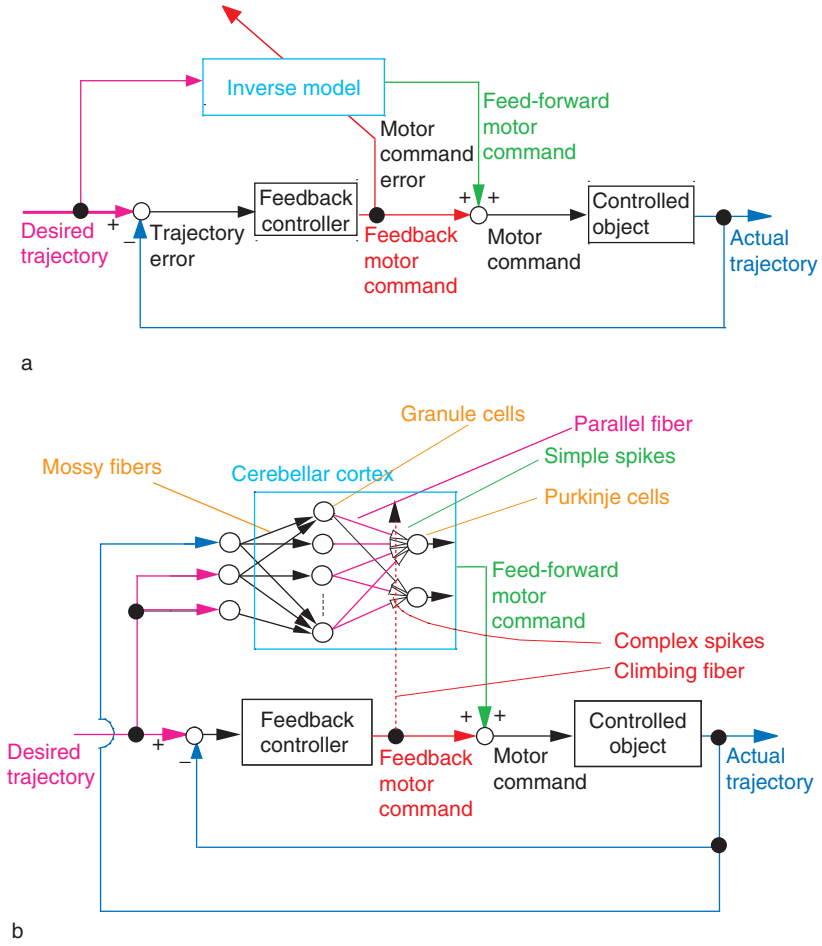

Figure 4 (a) The general feedback error learning model. (b) The cerebellar feedback error learning model. The 'controlled object' is a physical entity, such as the eyes, hands, legs, or torso, that needs to be controlled by the central nervous system. Different colors are for correspondence between (a) and (b).

almost absent in simple gain control with one degree of freedom, such as vestibulo-ocular reflex; thus, it motivated the following more recent models for general many-degrees-of-freedom movements with dynamics and kinematics. Several computational models have been proposed, such as direct inverse modeling, back-propagation through a forward model, or decorrelation learning, but the feedback error learning model, which transforms the sensory error into a motor error by a preexisting feedback controller in the central nervous system (Figure 4(a)), is probably the most biologically plausible and best supported.

The feedback error learning model depicted in Figure 4(a) is the same as the basic model shown in Figure 1 except for the following four points. First, the inverse model transforms a desired trajectory into a feed-forward motor command. Second, a crude feedback controller generates feedback motor command from the sensory error. Third, the summation of the feed-forward and feedback motor commands is sent to the controlled object. Finally, and most important, the feedback motor command is used as the error signal for motor commands in supervised learning for acquisition of the inverse model (cf. Figures 1 and 4(a)). Stability and convergence of the feedback error learning algorithm have been mathematically proved as well as successfully applied to several robotic demonstrations. Figure 4(b) adapts the basic feedback error learning model to the cerebellar neural circuit. Here, simple spikes represent feed-forward motor commands, and parallel fiber inputs represent the desired trajectory as well as the sensory feedback of the current status of the controlled object. A microzone of the cerebellar cortex constitutes (a part of) an inverse model of a specific controlled object such as the eye or arm. Most importantly, climbing fiber inputs are assumed to carry a copy of the feedback motor commands generated by the feedback control circuit. Thus, the complex spikes are predicted to be trajectory error signals already expressed in motor command coordinates. Although

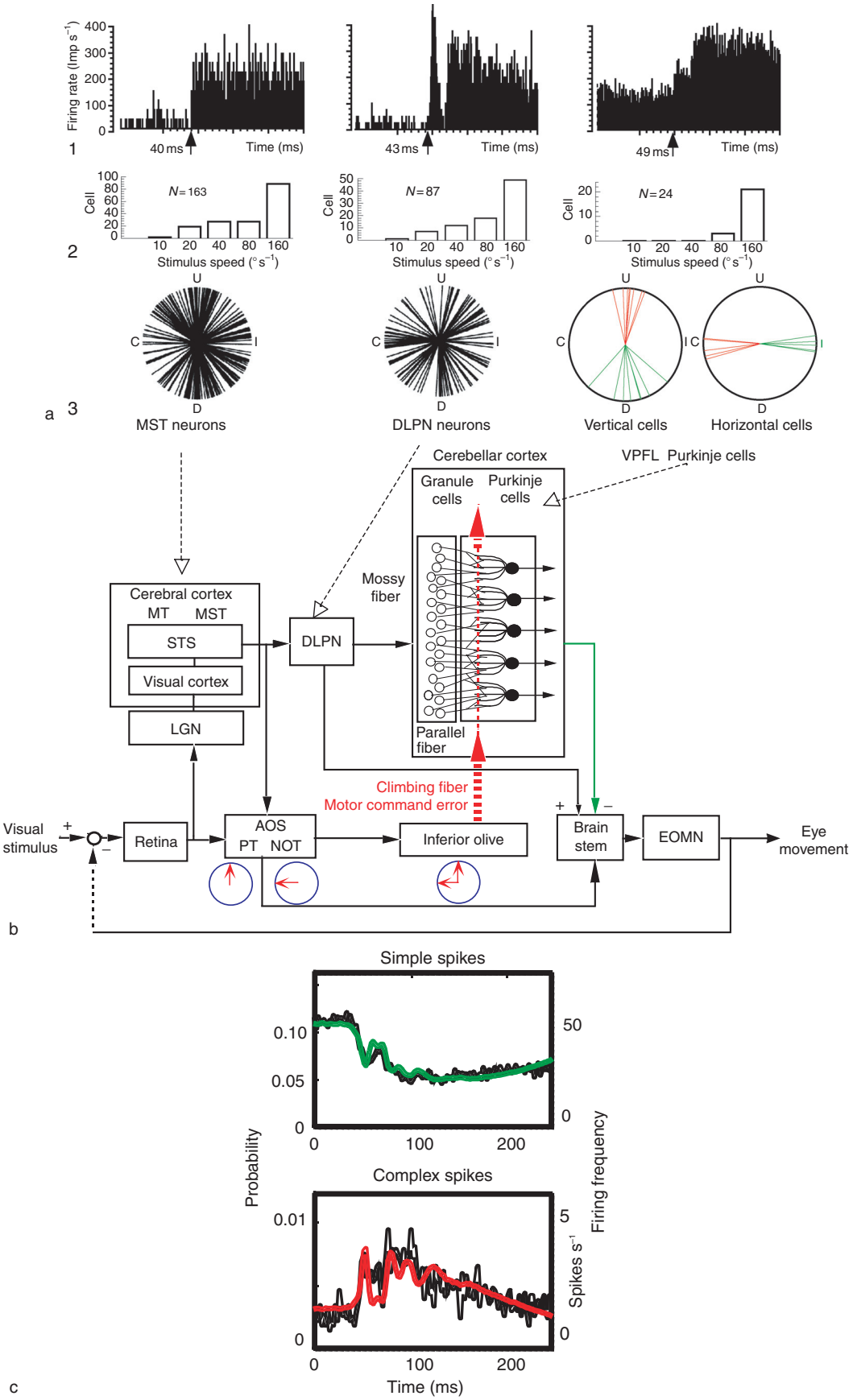

Figure 5 Continued

climbing fiber inputs are delayed by 100 ms with respect to the responsible parallel fiber inputs that caused the movement and the resulting error, spike timing dependency of LTD (see the section titled 'Computational models of cerebellar LTD') selectively changes only the responsible parallel fiber synapses.

The Ventral Paraflocculus and Ocular Following Responses

Kawano and his colleagues supported the cerebellar feedback error learning model by neurophysiological studies in the ventral paraflocculus of monkey cerebellum during ocular following responses. Ocular following responses are tracking movements of the eyes, evoked by movements of a large visual scene, that are thought to be important for the visual stabilization of gaze. In the neural circuit controlling this response Figure 5(b), the phylogenetically older, crude feedback circuit comprises the retina, the accessory optic system, and the brain stem. The phylogenetically newer and more sophisticated feed-forward pathway and the inverse dynamics model correspond to the cerebral and cerebellar cortical pathway and the cerebellum, respectively. In Figure 5(b), the sensory error signal is computed as the image motion on the retina (retinal slip). This is different from the schemes of Figures 1 and 4 in which some neural mechanisms explicitly compute the difference (error) between the desired and actual states. However, in the case of eye movement control such as ocular following responses or vestibulo-ocular reflexes, the desired state is that the eye movement is made so that the retinal image does not move, and thus the optical computation (retinal slip detection) can replace subtraction of the desired and actual states. On the other hand, the desired trajectory information transmitted to the flocculus for the vestibulo-ocular reflex is the head motion signal detected by semicircular canals whereas for the ocular following responses, it is the image motion signal conveyed by the visual areas in the cerebral cortex.

During ocular following responses, the time courses of simple spike firing frequency show complicated patterns (Figure 5(c) top, thin line). However, they were quite accurately reconstructed by using an inverse dynamics representation of eye movement (thick line). The model fit was good for the majority of the neurons studied under a wide range of visual stimulus conditions, different eye movements, and different firing patterns. The same inverse dynamics analysis for the medial superior temporal area (MST) of the cerebral cortex and dorsolateral pontine nucleus, which provide visual mossy fiber inputs, revealed that their firing time courses were not well reconstructed from motor commands but rather that they were well reconstructed from visual retinal slip. Taken together, these data suggest that the ventral paraflocculus is the major site of the inverse dynamics model of the eye for ocular following responses.

Motor commands, conveyed by simple spikes, should be directly modified and acquired by LTD while guided by motor command errors, which are conveyed by climbing fiber inputs. For this to work, the climbing fiber inputs need to convey comparable details of temporal and spatial information to the motor commands, but the ultralow discharge rates of the latter would appear to rule out this possibility. This apparently discrete and sporadic nature of climbing fiber inputs was characterized as an unexpected event detector, which suggested a reinforcement learning type theory. However, if thousands of

Figure 5 Change of neural codes and learning of inverse dynamics model in the cerebellum for ocular following responses (OFR). (a) Firing characteristics of medial superior temporal area (MST), dorsolateral pontine nucleus (DLPN), and ventral paraflocculus (VPFL) neurons. (b) Schematic neural circuit for OFR. (c) Temporal firing patterns of VPFL Purkinje cells in upward eye movements induced by upward visual motion. (a) The left, middle, and right columns are for MST, DLPN, and VPFL neurons, respectively. (1) Poststimulus-time histograms of the firing rates of a typical neuron in each of the three areas. The origin of time is the onset of visual stimulus motion. (2) Histograms of a number of cells within a given range of the optimum stimulus speeds. (3) Polar plots of optimum stimulus directions. U, C, D, and I, upward, contralateral, downward, and ipsilateral, respectively. VPFL Purkinje cells were classified into two groups: vertical cells and horizontal cells, based on simple spike (a dotted line) and complex spike (actual line) optimum directions. (b) The circuit can be divided into two main pathways. The upper part shows the corticocortical (the cerebral cortex to the cerebellar cortex) pathway, which corresponds to the feed-forward arc of feedback error learning. The lower part shows the phylogenetically older feedback pathway containing the accessory optic system (AOS), which corresponds to a crude feedback controller in the feedback error learning scheme. (c) Temporal firing patterns of nine accumulated Purkinje cells (thin curves) and their reconstruction based on inverse dynamics model (bold curves). The model predicts that the temporal firing patterns of simple spikes (upper pane) and complex spikes (lower pane) should be mirror images of each other, and this was confirmed experimentally. PT, pretectum; NOT, nucleus of optic tract; MT, middle temporal area; STS, superior temporal sulcus; LGN, lateral geniculate nucleus; EOMN, extraocular motor neurons. Adapted from Kawano K (1999) Ocular tracking: Behavior and neurophysiology. *Current Opinion in Neurobiology* 9: 467–473; Takemura A, Inoue Y, Gomi H, Kawato M, and Kawano K (2001) Change in neuronal firing patterns in the process of motor command generation for the ocular following response. *Journal of Neurophysiology* 86: 1750–1763; Kobayashi Y, Kawano K, Takemura A, et al. (1998) Temporal firing patterns of Purkinje cells in the cerebellar ventral paraflocculus during ocular following responses in monkeys. II. Complex spikes. *Journal of Neurophysiology* 80: 832–848. Reproduced from Kawato M (1999) Internal models for motor control and trajectory planning. *Current Opinion in Neurobiology* 9: 718–727, with permission from Elsevier.

trials are averaged, the firing rates actually conveyed very accurate and reliable time courses of motor command error within a few hundreds of milliseconds (Figure 5(c), bottom). More specifically, complex spike time courses are better reconstructed by retinal slip than by eye movements but in the motor command coordinates rather than in visual coordinates, as detailed below. Because LTD is a rather slow process, taking several tens of minutes, it can conduct the averaging over many trials. Consequently, the firing probability of climbing fiber inputs can convey high-frequency temporal information matching information of the dynamic command signal.

The preferred directions of MST and pontine neurons were evenly distributed over 360°, as shown in Figure 5(a)(3). Thus, the visual coordinates are uniformly distributed over all possible directions. On the other hand, projections of the three-dimensional spatial coordinates of the extraocular muscles were in either a horizontal or vertical direction, and they were entirely different from the visual coordinates. Preferred directions of simple spikes were either downward or ipsiversive (Figure 5(a)(3)), and at the site of each recording, electrical stimulation of a Purkinje cell elicited eye movement toward the preferred direction of the simple spike. These data indicate that the simple spike coordinate framework is already that of the motor commands. Thus, at the parallel fiber–Purkinje cell synapse, a drastic visuomotor coordinate transformation occurs. The neural representation dramatically changes from population coding in the MST and pontine nucleus to firing rate coding of Purkinje cells at the parallel fiber–Purkinje cell synapse (Figure 5(a)). What, then, is the origin of this drastic transformation? The theory proposes that the complex spikes, and ultimately the accessory optic system, are the source of this motor command spatial framework. The preferred directions of pretectum neurons are upward, and those of the contralateral nucleus of optic tract neurons are ipsiversive (thus contraversive for the cerebellum). Their signals are conveyed to the inferior olive and further to the cerebellum to produce the complex spikes. In summary, the coordinate frame of the climbing fibers was vertical and horizontal, forming the motor coordinates, not the visual coordinates of MST or pontine nucleus. All these experimental findings were successfully simulated by the network model shown in Figure 5(b). The coordinates of semicircular canals and the extraocular muscles are very similar, and it is rather difficult to evaluate coordinate transformation in the vestibulo-ocular reflex and flocculus compared with ocular following responses. However, recent physiological studies indicate that climbing fiber inputs encode motor error rather than sensory error. This argues against a class of model that assumes sensory–motor transformation downstream of Purkinje cells, including decorrelation models.

Toward a General Model of the Cerebellum

We have a very solid computational model (feedback error learning and inverse model) and a rich set of supporting experimental data for the ventral paraflocculus with ocular following responses. The model has also been well supported for other slow eye movements, such as vestibulo-ocular reflex, optokinetic eye movements, and smooth pursuit, for the flocculus and paraflocculus. Can we extend this to other parts of the cerebellum, other types of movements, and other computational models? Many theorists believe so since the neural circuit is generally uniform except for the newly found unipolar brush cells, found primarily in the flocculonodular lobe. Furthermore, Kitazawa and colleagues have demonstrated that complex spikes recorded from cerebellar hemispheres encode reaching errors at goal points during monkey whole-arm reaching, whereas simple spikes represent movement dynamics such as an electromyogram.

What can we generalize about cerebellar functions from previous studies on specific functions and specific areas? First, synaptic plasticity is unique and ubiquitous, and the learning is undoubtedly supervised learning and not Hebbian or reinforcement learning. Second, the cerebellar 100 ms STDP, in contrast to cerebral and hippocampal millisecond-order STDP, strongly suggests that the cerebellum is better suited for approximating some nonlinear dynamical system outside the cerebellum as 100 ms is exactly the time required for sensory signal feedback from the external world. Finally, the major computation is feed-forward, with less emphasis on recurrent feedback, because spatial resources are allocated more to neurons than to their connections in the cerebellum, as is evident from the number of neurons: more than that of the cerebrum in a volume only one-tenth that of the cerebrum. Consequently, internal models are the most promising computational functions of the cerebellum. Forward models have been theoretically postulated several times and supported by neuroimaging experiments. Cancellation of a self-generated electrical field by a forward model is the function of the electrosensory lobe (cerebellum-like structure) of the weakly electric fish and might be interpreted as another support. But it is actually a different story because NMDA receptors play the essential role in anti-Hebbian learning there. Thus, supporting evidence

for forward models is much more circumstantial than is the evidence for inverse models, and we need more-decisive data. Computational models for how multiple internal models are integrated and used for motor control and cognition have been proposed (e.g., the modular selection and identification for control model), but innovative experimental methodology to further explore these phylogenetically newer functions of the cerebellum seems necessary.

See also: Cerebellar Microcircuitry; Cerebellar Deep Nuclei; Cerebellum and Oculomotor Control; Cerebellum: Clinical Pathology; Cerebellum: Evolution and Comparative Anatomy; Olivocerebellar System; Procedural Learning: Cerebellum Models; Sporadic Degenerative Ataxias and the Dominantly Inherited Spinocerebellar Ataxias.

Further Reading

Albus JS (1971) A theory of cerebellar function. *Mathematical Biosciences* 10: 25–61.

Daniel H, Levenes C, and Crepel F (1998) Cellular mechanisms of cerebellar LTD. *Trends in Neurosciences* 21: 401–407.

Dean P, Porrill J, and Stone JV (2002) Decorrelation control by the cerebellum achieves oculomotor plant compensation in simulated vestibulo-ocular reflex. *Proceedings of the Royal Society of London, Series B: Biological Sciences* 269: 1895–1904.

De Schutter E (1995) Cerebellar long-term depression might normalize excitation of Purkinje cells: A hypothesis. *Trends in Neurosciences* 18: 291–295.

De Schutter E (1999) Using realistic models to study synaptic integration in cerebellar Purkinje cells. *Reviews in the Neurosciences* 10: 233–245.

Doi T, Kuroda S, Michikawa T, and Kawato M (2005) Inositol 1,4,5-trisphosphate-dependent Ca^{2+} threshold dynamics detect spike timing in cerebellar Purkinje cells. *Journal of Neuroscience* 25: 950–961.

Fujita M (1982) Adaptive filter model of the cerebellum. *Biological Cybernetics* 45: 195–206.

Gomi H, Shidara M, Takemura A, et al. (1998) Temporal firing patterns of Purkinje cells in the cerebellar ventral paraflocculus during ocular following responses in monkeys. I. Simple spikes. *Journal of Neurophysiology* 80: 818–831.

Imamizu H, Miyauchi S, Tamada T, et al. (2000) Human cerebellar activity reflecting an acquired internal model of a new tool. *Nature* 403: 192–195.

Ito M (1970) Neurophysiological basis of the cerebellar motor control system. *International Journal of Neurology* 7: 162–176.

Ito M (1984) *The Cerebellum and Neural Control.* New York: Raven Press.

Ito M (2006) Cerebellar circuitry as a neuronal machine. *Progress in Neurobiology* 78: 272–303.

Ivry RB and Spencer RM (2004) The neural representation of time. *Current Opinion in Neurobiology* 14: 225–232.

Jordan MI and Rumelhart DE (1992) Forward models: Supervised learning with a distal teacher. *Cognitive Science* 16: 307–354.

Kawano K (1999) Ocular tracking: Behavior and neurophysiology. *Current Opinion in Neurobiology* 9: 467–473.

Kawato M (1999) Internal models for motor control and trajectory planning. *Current Opinion in Neurobiology* 9: 718–727.

Kawato M, Furukawa K, and Suzuki R (1987) A hierarchical neural-network model for control and learning of voluntary movement. *Biological Cybernetics* 57: 169–185.

Kawato M and Gomi H (1992) The cerebellum and VOR/OKR learning models. *Trends in Neurosciences* 15: 445–453.

Keating JG and Thach WT (1995) Nonclock behavior of inferior olive neurons: Interspike interval of Purkinje cell complex spike discharge in the awake behaving monkey is random. *Journal of Neurophysiology* 73: 1329–1340.

Kitazawa S and Wolpert DM (2005) Rhythmicity, randomness and synchrony in climbing fiber signals. *Trends in Neurosciences* 28: 611–619.

Kitazawa S, Kimura T, and Yin PB (1998) Cerebellar complex spikes encode both destinations and errors in arm movements. *Nature* 392: 494–497.

Kobayashi Y, Kawano K, Takemura A, et al. (1998) Temporal firing patterns of Purkinje cells in the cerebellar ventral paraflocculus during ocular following responses in monkeys. II. Complex spikes. *Journal of Neurophysiology* 80: 832–848.

Kuroda S, Schweighofer N, and Kawato M (2001) Exploration of signal transduction pathways in cerebellar long-term depression by kinetic simulation. *Journal of Neuroscience* 21: 5693–5702.

Lang EJ, Sugihara I, and Llinas R (1996) GABAergic modulation of complex spike activity by the cerebellar nucleoolivary pathway in rat. *Journal of Neurophysiology* 76: 255–275.

Llinas R, Lang EJ, and Welsh JP (1997) The cerebellum, LTD, and memory: Alternative views. *Learning & Memory* 3: 445–455.

Llinas R and Yarom Y (1986) Oscillatory properties of guinea-pig inferior olivary neurones and their pharmacological modulation: An *in vitro* study. *Journal of Physiology* 376: 163–182.

Marr D (1969) A theory of cerebellar cortex. *Journal of Physiology (London)* 202: 437–470.

Miall RC, Weir DJ, Wolpert DM, and Stein JF (1993) Is the cerebellum a Smith Predictor? *Journal of Motor Behavior* 25: 203–216.

Ogasawara H, Doi T, Doya K, and Kawato M (2007) Nitric oxide regulates input specificity of long-term depression and context dependence of cerebellar learning. *PLoS Computational Biology* 3(1): e179 doi:10.1371/journal.pcbi.0020179.

Schweighofer N, Doya K, Fukai H, Chiron JV, Furukawa T, and Kawato M (2004) Chaos may enhance information transmission in the inferior olive. *Proceedings of the National Academy of Sciences of the United States of America* 101: 4655–4660.

Shidara M, Kawano K, Gomi H, and Kawato M (1993) Inverse-dynamics model eye movement control by Purkinje cells in the cerebellum. *Nature* 365: 50–52.

Shutoh F, Ohki M, Kitazawa H, Itohara S, and Nagao S (2006) Memory trace of motor learning shifts transsynaptically from cerebellar cortex to nuclei for consolidation. *Neuroscience* 139: 767–777.

Takemura A, Inoue Y, Gomi H, Kawato M, and Kawano K (2001) Change in neuronal firing patterns in the process of motor command generation for the ocular following response. *Journal of Neurophysiology* 86: 1750–1763.

Yamamoto K, Kobayashi Y, Takemura A, Kawano K, and Kawato M (2002) Computational studies on acquisition and adaptation of ocular following responses based on cerebellar synaptic plasticity. *Journal of Neurophysiology* 87: 1554–1571.